SOLAR AND WASTE HEAT DESALINATION BY MEMBRANE DISTILLATION

College of Engineering
University of Texas at El Paso
El Paso, TX 79968

Agreement No. 98-FC-81-0048

Desalination and Water Purification Research and Development Program Report No. 81

April 2004

U.S. Department of the Interior
Bureau of Reclamation
Denver Office
Technical Service Center
Environmental Services Division
Water Treatment Engineering and Research Group

REPORT DOCUMENTATION PAGE

Form Approved
OMB No. 0704-0188

1. AGENCY USE ONLY *(Leave Blank)*	2. REPORT DATE	3. REPORT TYPE AND DATES COVERED
	April 2004	Final

4. TITLE AND SUBTITLE

Solar and Waste Heat Desalination by Membrane Distillation

5. FUNDING NUMBERS

Agreement No. 98-FC-81-0048

6. AUTHOR(S)

John Walton, Huanmin Lu, Charles Turner, Sergio Solis and Herbert Hein

7. PERFORMING ORGANIZATION NAME(S) AND ADDRESS(ES)

College of Engineering
University of Texas at El Paso
El Paso, TX 79968

8. PERFORMING ORGANIZATION REPORT NUMBER

9. SPONSORING/MONITORING AGENCY NAME(S) AND ADDRESS(ES)

Bureau of Reclamation
Denver Federal Center
P.O. Box 25007
Denver, CO 80225-0007

10. SPONSORING/MONITORING AGENCY REPORT NUMBER

DWPR No. 81

11. SUPPLEMENTARY NOTES

Desalination and Water Purification Research and Development (DWPR) Program

12a. DISTRIBUTION/AVAILABILITY STATEMENT

Available from the National Technical Information Service, Operations Division, 5285 Port Royal Road, Springfield, Virginia 22161

12b. DISTRIBUTION CODE

13. ABSTRACT ***(Maximum 200 words)***

In this study, the desalination performance and O&M procedures of an air-gap type membrane distillation system was tested using low-grade thermal energy (between 13 and 75 ºC) supplied by a salt-gradient solar pond. The research included measuring the flux per unit area of membrane surface and separation of ions over a range of feedwater salinities and temperature as well as an assessment of membrane fouling.

14. SUBJECT TERMS--

thermal desalination, solar pond, waste heat, membrane distillation, brackish groundwater

15. NUMBER OF PAGES

28 + appendices

16. PRICE CODE

17. SECURITY CLASSIFICATION OF REPORT	18. SECURITY CLASSIFICATION OF THIS PAGE	19. SECURITY CLASSIFICATION OF ABSTRACT	20. LIMITATION OF ABSTRACT
UL	UL	UL	UL

SOLAR AND WASTE HEAT DESALINATION BY MEMBRANE DISTILLATION

John Walton
Huanmin Lu
Charles Turner
Sergio Solis
Herbert Hein

College of Engineering
University of Texas at El Paso
El Paso, TX 79968

Agreement No. 98-FC-81-0048

Desalination and Water Purification Research and Development Program Report No. 81

April 2004

U.S. Department of the Interior
Bureau of Reclamation
Denver Office
Technical Service Center
Environmental Services Division
Water Treatment Engineering and Research Group

Mission Statements

U.S. Department of the Interior

The mission of the Department of the Interior is to protect and provide access to our Nation's natural and cultural heritage and honor our trust responsibilities to Indian tribes and our commitments to island communities.

Bureau of Reclamation

The mission of the Bureau of Reclamation is to manage, develop, and protect water and related resources in an environmentally and economically sound manner in the interest of the American public.

Federal Disclaimer

The information contained in this report regarding commercial products or firms may not be used for advertising or promotional purposes and is not to be construed as an endorsement of any product or firm by the Bureau of Reclamation.

ACKNOWLEDGMENTS

This research was sponsored by the Desalination and Water Purification Research and Development Program, Bureau of Reclamation. The University of Texas at El Paso (UTEP) Department of Civil Engineering wishes to thank Bruce Foods Corporation for providing space and facilities at the El Paso solar pond.

A number of undergraduate students from UTEP assisted in the project, including Becky Lozoya, Adam Lozoya, Hector Sepulveda, and Al Salcedo.

TABLE OF CONTENTS

TABLES

FIGURES

FIGURES

1.0 Introduction

1.1 Overview of Technology

Membrane distillation (MD) is an emerging technology for desalination. Membrane distillation differs from other membrane technologies in that the driving force for desalination is the difference in vapor pressure of water across the membrane, rather than total pressure. The membranes for MD are hydrophobic, which allows water vapor (but not liquid water) to pass. The vapor pressure gradient is created by heating the source water, thereby elevating its vapor pressure. The major energy requirement is for low-grade thermal energy.

A variety of methods have been employed to impose the vapor pressure difference across the hydrophobic membranes (Lawson and Lloyd, 1997). In every case, the raw water to be desalted directly contacts the hot side of the membrane. The four classes of membrane distillation are:

- **Direct-Contact Membrane Distillation**. The cool condensing solution directly contacts the membrane and flows countercurrent to the raw water. This is the simplest configuration. It is best suited for applications such as desalination and concentration of aqueous solutions (e.g., juice concentrates).

- **Air-Gap Membrane Distillation**. An air gap followed by a cool surface. The air gap configuration is the most general and can be used for any application.

- **Sweep-Gas Membrane Distillation**. A sweep gas pulls the water vapor and/or volatiles out of the system. Useful when volatiles are being removed from an aqueous solution.

- **Vacuum Membrane Distillation**. A vacuum is used to pull the water vapor out of the system. Useful when volatiles are being removed from an aqueous solution.

The advantages of membrane distillation are:

- It produces high-quality distillate.

- Water can be distilled at relatively low temperatures (0 to 100 °C).

- Low-grade heat (solar, industrial waste heat, or desalination waste heat) may be used.

- The water does not require extensive pretreatment as in pressure-based membrane treatment.

A schematic of an air-gap membrane distillation unit is shown in figure 1. The brackish or saline water to be distilled is heated and passed by one side of the membrane. Water vapor diffuses across the membrane and air gap to the other side, where it condenses on the cooler surface. The right side of the air gap is kept cool by a flow of cooling water. The overall process is driven by a gradient in water vapor pressure, rather than a difference in total pressure. Thermal energy is required to elevate the vapor pressure of water in the hot stream.

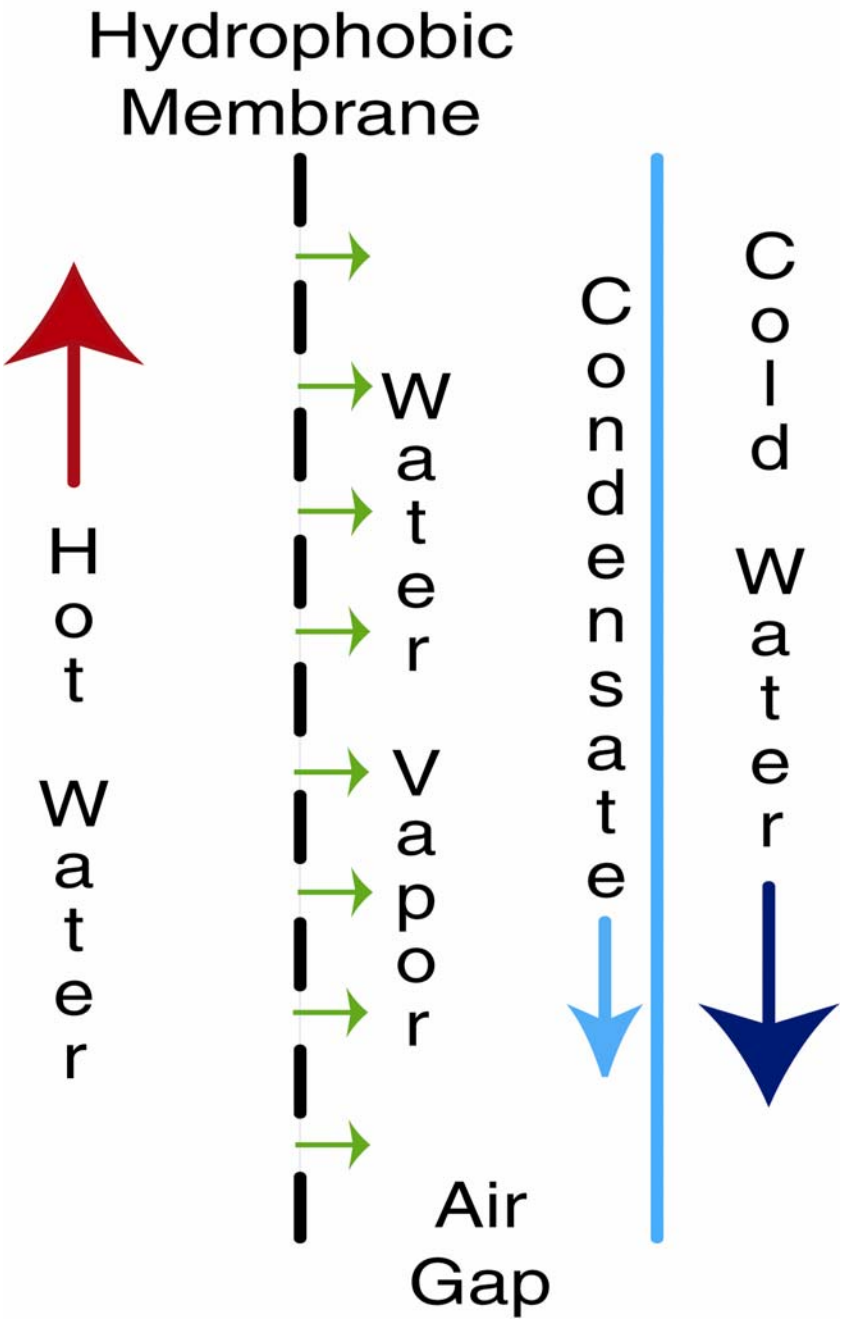

Figure 1. Schematic of air-gap membrane distillation.

The membrane itself is hydrophobic with pore sizes usually in the range of 0.05 to 0.2 μm—the same range as microfiltration. Lawson (1995), for example, used polypropylene membranes with maximum pore sizes ranging from 0.3 to 1.1 μm. Water is kept from penetrating the pores by surface tension and capillary pressure.

Membrane distillation has been investigated in very small-scale (a few cm^2 of membrane area) laboratory systems, but not on actual operating systems. The goal of this research was to test a small, commercially available MD module to gather data on flux, thermal efficiency, fouling, distillate quality, and operational characteristics.

1.2 Experimental Setup

The project was a collaboration with the Swedish firm SCARAB HVR <http://www.hvr.se>. SCARAB builds air-gap MD systems. An entire system (membrane module plus controlling pumps and heaters) built by SCARAB and previously tested at Sandia National Laboratory was obtained. (Robert Donovan, personal communication. A copy of Sandia's test results can be obtained by contacting Mr. Donovan at Sandia.) Preliminary testing was performed with the Sandia system, allowing operational experience to be gained while not risking damage to the new membrane module. The new membrane module was later plumbed and used to collect all data shown. Heating and cooling water were obtained from the El Paso solar pond.

An overall flow schematic is shown in figure 2. Hot brine was pumped from the bottom of the solar pond and passed through a heat exchanger to supply heat. Cold water from the solar pond surface was passed through a heat exchanger to provide cooling. High and low temperatures for system operation were obtained by changing the flow rates for solar pond hot and cold water. Hot water lines were made of CPVC, and cooling lines were made of PVC. Figure 3 is a picture of the modified SCARAB system. The membrane module is in the background; 2.94 m^2 of membrane are present in the module.

A series of thermocouple sensors and magnetic flowmeters was installed throughout the system on the heat exchangers, feed and return lines to the membrane, and in the recirculating cooling loop. Conductivity probes were installed in the make up water tank and in the distillate product line, in order to measure the source water to be tested and the quality of the distillate. All of the mentioned sensors and probes were connected to two signal acquisition boards (DBK Omega ™ series), which then were hooked to a computer via a data acquisition board (Daqboard from Omega ™). By using the latest version of the software DaqView®, data for temperature, flow, and conductivity were registered for later analysis. Details of the experimental setup are given in Solis (1999).

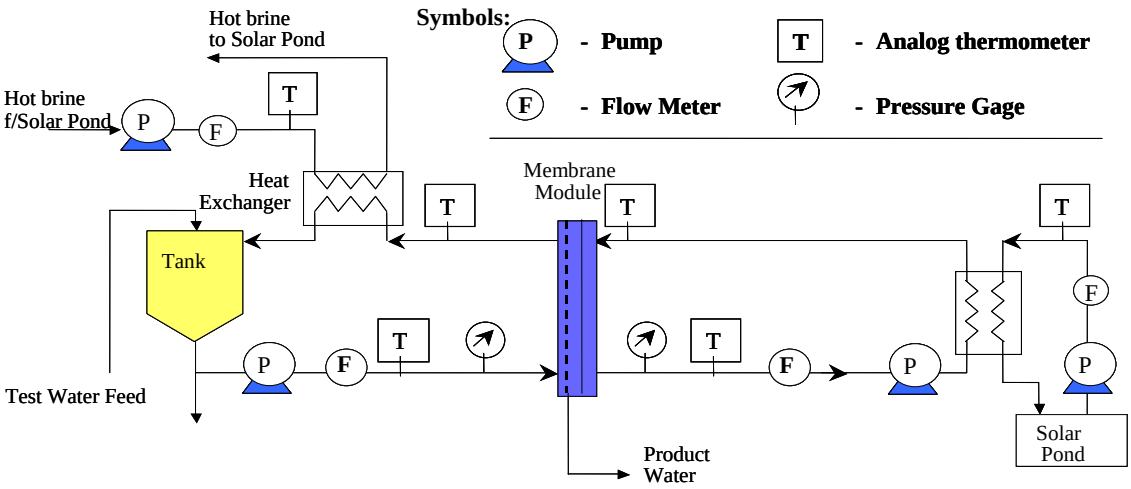

Figure 2. Flow schematic.

Figure 3. Modified SCARAB membrane distillation system.

1.3 Experimental Plan

The major purpose of the test matrix was to: (a) determine performance over this range of operational parameters; and (b) attempt to deduce controlling factors based upon experimental results. The secondary goal was to evaluate membrane fouling during desalination of local waters.

In September 1999, a sequential concentration test was performed using local ground water. Concentrate was recycled back into the source water tank to give sequentially more concentrated feed. This testing was part of the initial system shakedown.

During October and November 1999, an experimental matrix was performed with sodium chloride solutions. The data collected during these tests are presented in Appendices A through D at the back of this report. Flux and distillate quality were measured with varying input water salinity, hot side temperature, and temperature drop. Water properties for the test matrix are given in table 1.

Table 1. Properties of water tested in experimental matrix

NaCl concentration (molality)	Specific gravity at 20 °C	(%) salinity	Salt content (g/l)
0	1.000	0.0	0.0
0.6 (“seawater”)	1.025	3.50	35.7
2.0	1.083	1.5	124.4
3.0	1.118	16	178.6
4.0	1.171	23	269.6

Constant composition during each set of experiments was maintained by returning the distillate to the source tank. Hot side temperature and temperature drop could only be approximately controlled.

No pretreatment was provided for the water. Flows and temperatures were recorded directly by computer. During evaluation of the experimental matrix, distillate production was measured by hand into a volumetric flask. This was required because the automated flow measurement system was not sufficiently accurate at low flow rates.

2.0 Conclusions and Recommendations

2.1 Conclusions

- Flux per unit area of membrane surface ranges from 0 to 6 L/m^2/hr. Flux increases linearly with transmembrane temperature drop, decreases significantly with increasing salinity for brines, and depends only weakly on hot side temperature.

- The data indicate that flux is heat transfer limited and only weakly responsive to vapor pressure gradients between the feed water and cooling water. This is a surprising conclusion for air gap membrane distillation where diffusional mass transport of water vapor across the membrane and air gap is anticipated to control flux.

- Flux was measured down to hot side temperatures as low as 13 ºC. Flux per unit temperature drop at very low temperatures was only reduced about 50 percent compared to flux at higher temperatures. Operation of MD at such low temperatures may open up thermal energy resources that have not previously been considered for desalination.

- The low dependence of flux on hot side temperature and continuation of flux at very low temperatures mean that the technology can take advantage of low-grade heat energy.

- Very high quality distillate can be produced even from nearly saturated NaCl brine. Distillate quality is primarily dependent upon the degree of wetting of the membrane. Pressure spikes or lack of temperature gradient can lead to wetting of some pores and subsequent decline in distillate quality.

- The hydrophobic properties of the membrane can be restored by simple drying. An ordinary hair dryer was used periodically for this purpose.

- The fraction of the heat supplied that went into distillation ranged from over 90 percent for low salinity water to around 50 percent for concentrated brine. The membrane module tested was not designed to recover latent heat. This is not a limitation of the technology but, rather, a limitation of current production modules.

- Theoretical calculations, based upon measured results, indicate that membrane distillation with latent heat recovery can be easily implemented and that this modification would make MD competitive with other thermal technologies in terms of energy use.

2.2 Recommendations

- Leakage rate through wetted pores is proportional to pressure drop. If the hot water passing through the membrane module were kept near atmospheric pressure, the rate of leakage through wetted pores would be reduced to near zero. This would ensure high distillate quality even when water begins to penetrate the membrane pores.

- Damaging pressure spikes could be eliminated by changing the overall system to provide gravity flow (high tank to low tank) through the membrane module.

- A countercurrent flow system would provide greater energy efficiency at the cost of lower flux per unit area of membrane (i.e., higher capital costs).

- In the short term, the greatest promise for MD is for isolated low technology (village) applications, ships, and the military.

- Membrane distillation may also be competitive in treating reverse osmosis (or nanofiltration) concentrate.

- Longer-term tests are required to quantify fouling. No membrane fouling was detected during the tests performed on sodium chloride solutions and concentrated local ground waters.

- Alternative sources of low-grade thermal energy should be considered for use with MD desalination, such as wet bulb/dry bulb temperature differences, thermally stratified waters, and ground/air temperature differences.

3.0 Results

3.1 Flux

In order to better understand the relative role of salt content, hot side temperature, and temperature drop, initial tests were performed using previously distilled water as the raw water supply. Flux results for distillation of essentially pure water are shown in figure 4. The different symbols represent different ranges of hot side temperatures. The setup of the system precluded very precise temperature control, making it necessary to lump the data into ranges. In these experiments, the flow rate of recirculating water was nominally held at 20 L/min. Flux increases linearly with hot to cold side temperature drop and increases only weakly with higher hot side temperatures. Visual extrapolation of the data at the low end indicates that flux begins as soon as an infinitesimal temperature drop is created. Comparison of fluxes is only available in the published literature from small laboratory systems using a few cm^2 of membrane area. Godino, *et al*. (1996), obtained fluxes up to 12 $L/m^2/hr$ in a laboratory direct contact MD test with a temperature drop of 50 ºC. Lawson (1996) obtained up to 68 $L/m^2/hr$ in a laboratory direct contact membrane distillation test when the temperature drop was 40 ºC. Lawson used new, higher flux membranes from 3M Company, as well as an experimental apparatus with high Reynolds numbers (less temperature polarization). Ohta, *et al*. (1991), obtained fluxes of up to 5.5 $L/m^2/hr$ with a direct contact laboratory system. Direct contact systems should have a higher flux and lower thermal efficiency relative to air gap systems.

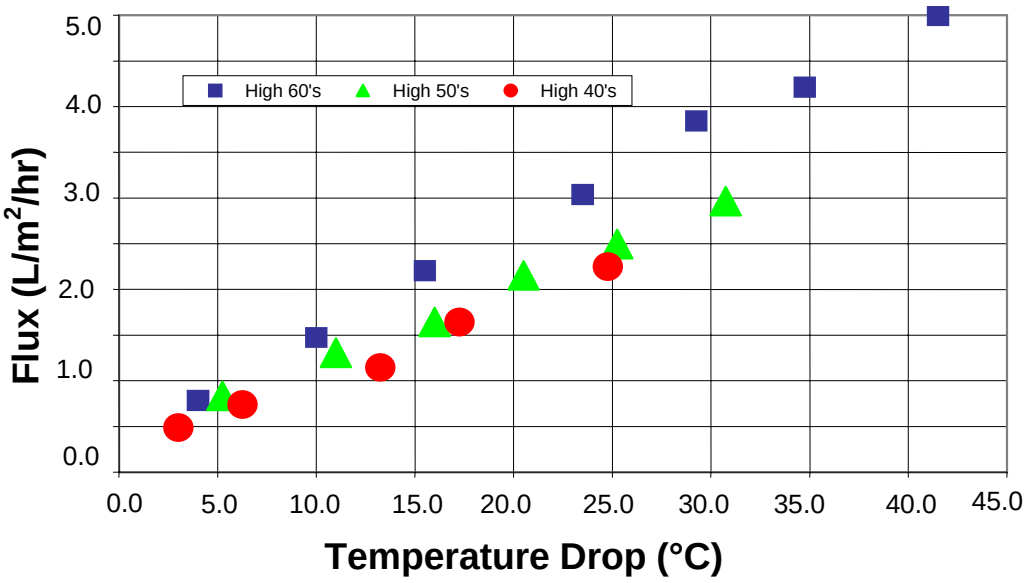

Figure 4. Production as a function of hot side temperature and temperature drop for pure water.

Flux at 0.6 M input water NaCl concentration (nominally seawater strength), as shown in figure 5, exhibits the same trends. The major differences are: (a) slightly lower flux at any point; and (b) initiation of flux requires at least 2 to 3 ºC temperature drop.

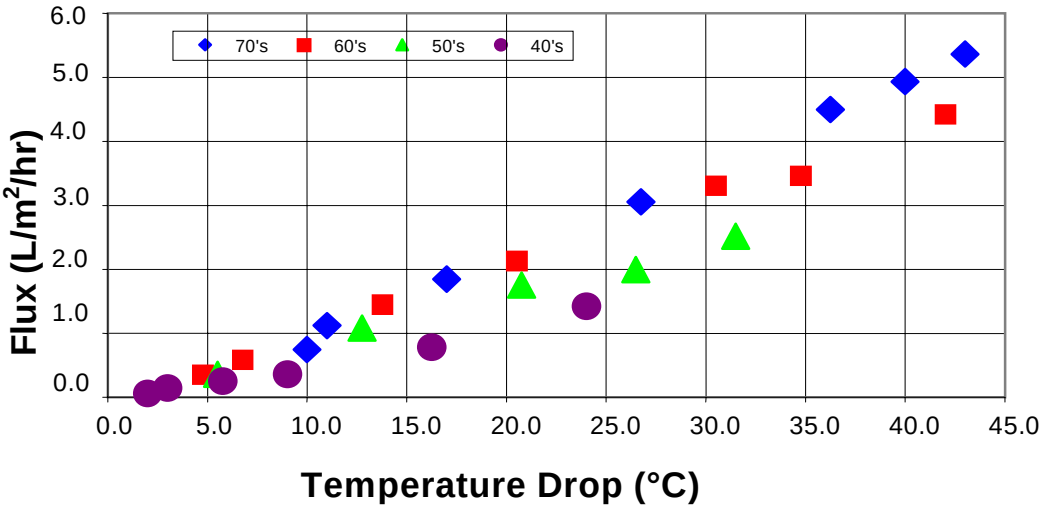

Figure 5. Production as a function of hot side temperature and temperature drop for 0.6 molar water

Figure 6 gives flux at 0, 0.6, 2, and 4 input water NaCl molality for hot side temperatures between 60 and 70 ºC. Flux declines markedly at very high brine concentrations. The temperature drop required to initiate flux (i.e., the x-axis intercept) also increases with brine content of the source water.

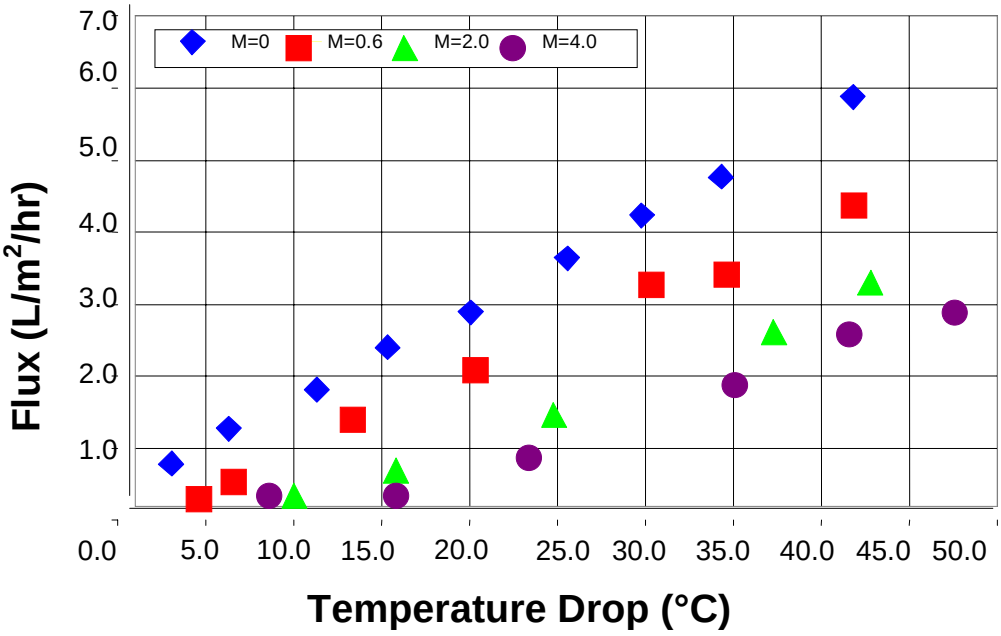

Figure 6. Flux at 50 to 60 °C hot side temperature as a function of molality.

Figure 7 illustrates the influence of the flow rate of the hot side recirculating water. Higher flow rates create greater turbulence (higher Reynolds numbers), which leads to greater heat transfer. Higher water flow rate has a small but significant influence on flux, especially at higher flux rates associated with high temperature drops.

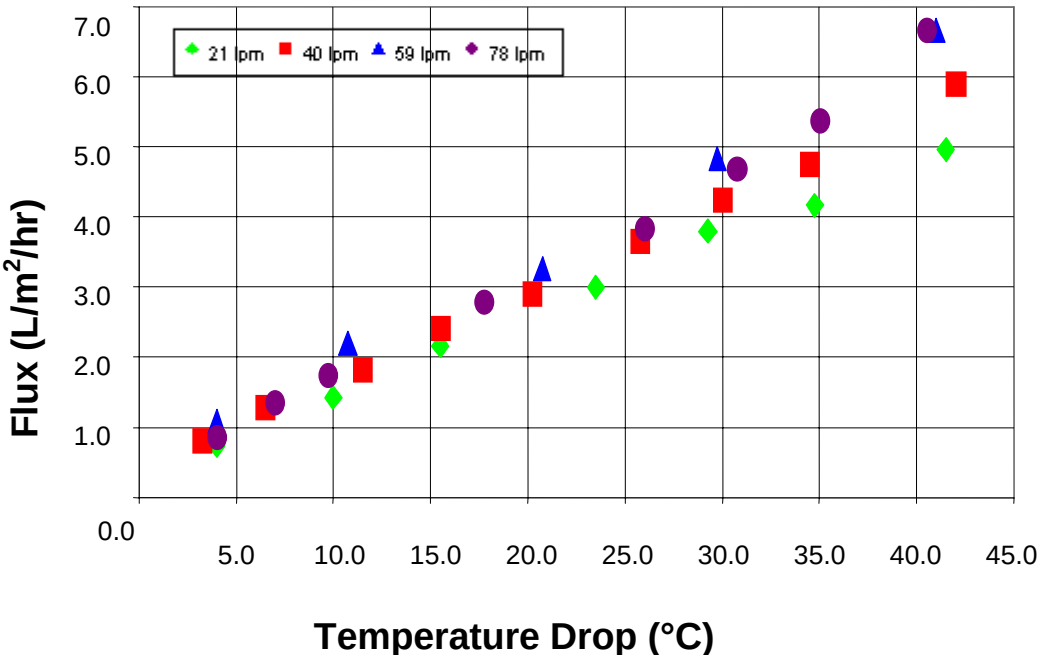

Figure 7. Influence of recirculating water flow rate.

An important question is how the system performs at low temperatures. In the above flux graphs, the hot side temperatures were held approximately constant while the cold side temperature was varied. In order to investigate low temperature performance, this procedure was reversed: the cold side temperature was held approximately constant while the hot side temperature was lowered from 36.5 ºC down to 12.9 ºC. The low temperature results are compared with higher temperature results in figure 8. At a hot side temperature of 12.9 ºC and a temperature drop of only 1.5 ºC, a measurable flux of 0.08 L/m^2/hr was measured. Comparison of the trendlines demonstrates that hot side temperatures in the range of 13 to 36 ºC produce about half the flux of hot side temperatures in the range of 60 to 70 ºC at the same temperature drop.

3.2 Energy

Energy performance is shown in figure 9. The economy ratio is defined as the ratio of the heat energy theoretically required to distill the measured flux of water divided by the total heat energy used by the system. The economy ratio was calculated only for the highest temperature drops where flux was greatest. The system design has high flow rates of hot and cold water passing through the module, with small temperature changes between input and output flows. For this reason, a high uncertainty is associated with the measured energy balance, especially at lower flux rates.

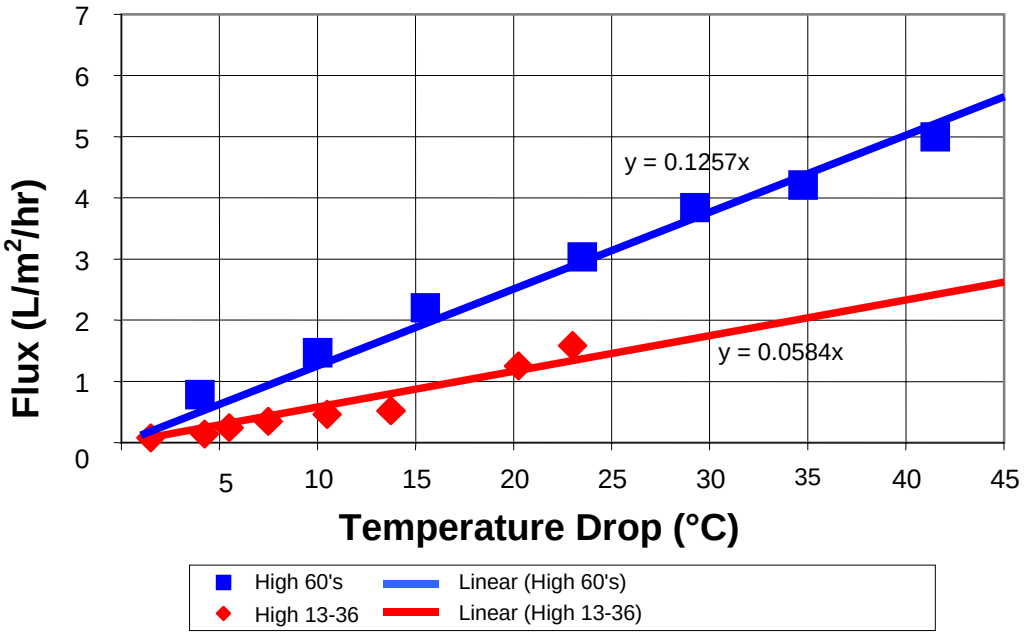

Figure 8. Comparison of performance at low temperatures.

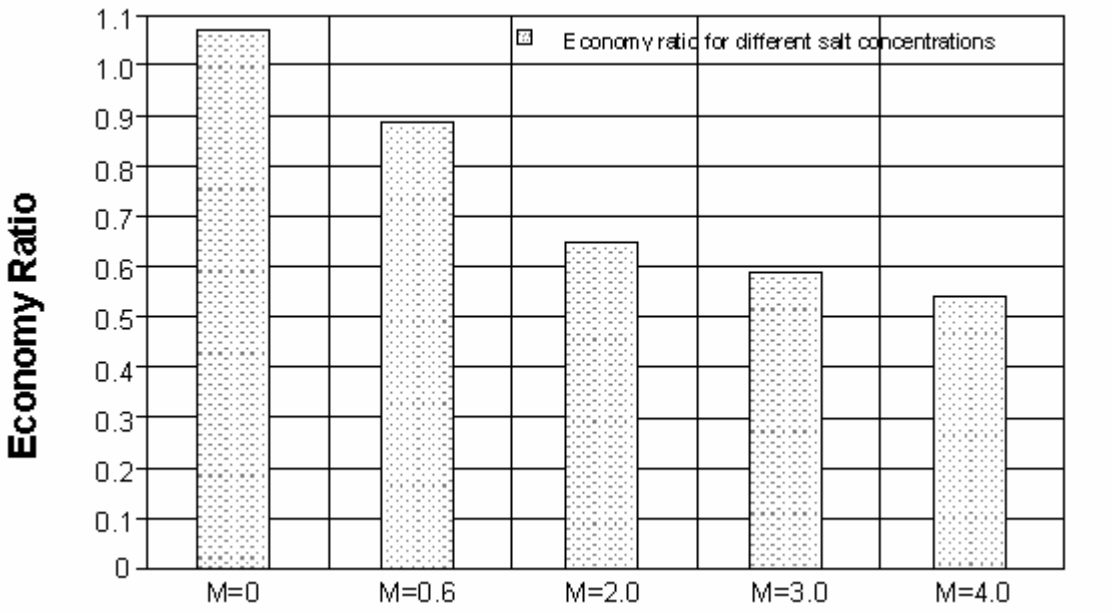

Figure 9. Economy ratio as influenced by molality.

Figure 9 shows decreasing energy efficiency as the brine becomes more concentrated. The membrane module tested was not designed to recover latent heat and should have a theoretical maximum economy ratio of one. We have been unable to find any published, measured,

energy efficiency data for membrane distillation. Based upon first principles, air gap membrane distillation should be more energetically efficient than direct contact membrane distillation.

Although fluxes are lower (meaning capital costs would increase), MD can be used to desalinate water at very low hot side temperatures (down to at least 13 ºC).

3.3 Quality - Wetting of the Membrane

The hydrophobic nature of the membrane separates the brackish, warm water from the air gap. For simplicity, only one pore is shown in the hydrophobic membrane in figure 10. The water "bulges" through the pore until the surface tension and radius of curvature create a force to exactly balance the pressure drop across the membrane. This force per unit area, which is equal to the pressure drop across the membrane, is called the capillary pressure.

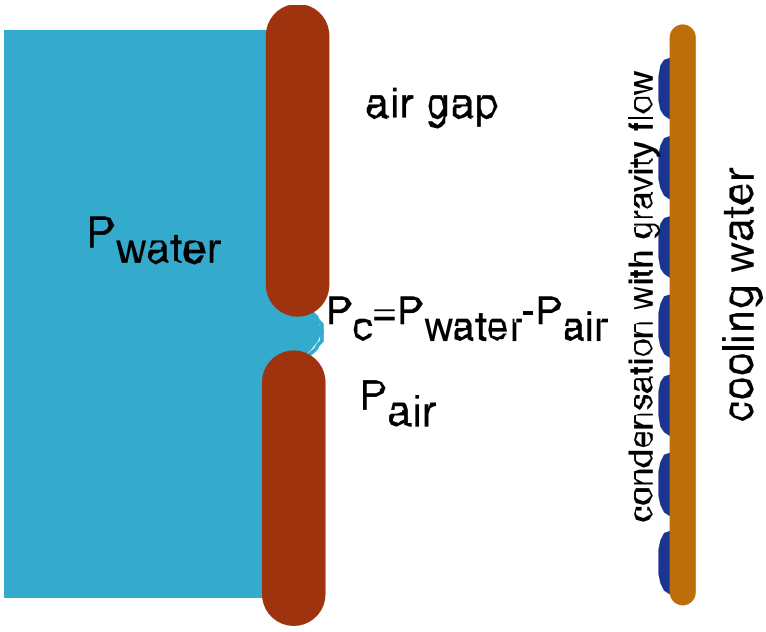

Figure 10. Capillary pressure.

The maximum radius of curvature and, thus, maximum capillary pressure prior to leakage of liquid water across the membrane depend upon pore size and surface tension. When the surface tension forces are overwhelmed, the pore begins leaking. Once a pore begins leaking, the membrane may locally lose its hydrophobic properties, leading to constant leaking at any water/air pressure differential (Banat, *et al*., 1994). Surface tension and viscosity of water decline with temperature (Chemical Rubber Company, 1970), making leakage a greater potential problem at higher temperatures.

Portions of the membrane that become wet leak, based upon the total pressure drop across the membrane. For experiments where the water recirculating flow rate was not changed, the rate of leakage was approximately constant. As the flux increases, the leaking water is diluted by distillate, which leads to better water quality. An example is shown in figure 11. The rate of

leakage through the membrane can be calculated from the conductivity of the source and distilled water. All reported fluxes in this report were corrected for membrane leakage rates.

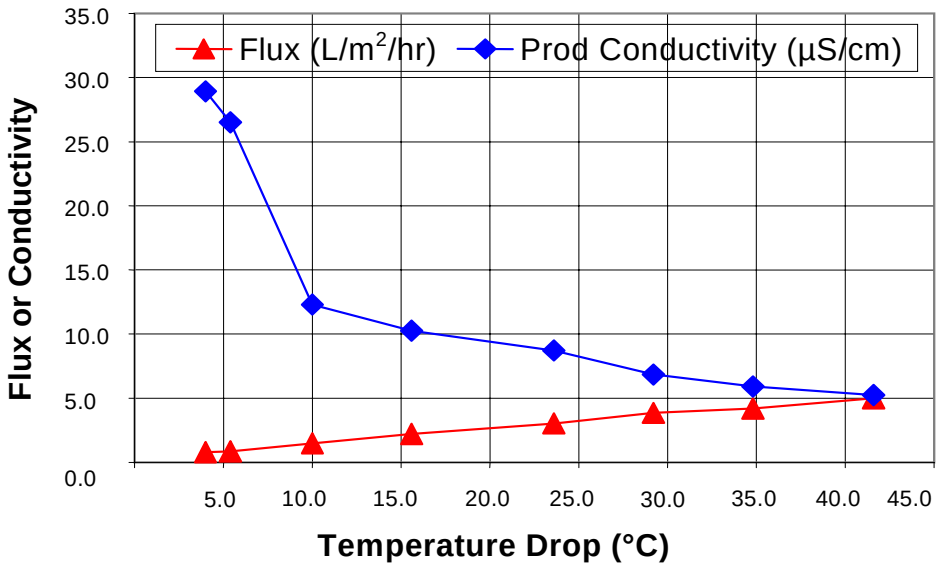

Figure 11. Quality as influenced by flux.

The history of membrane leakage is plotted in figure 12. The bars give calculated leakage rate, and the salinity of the source water being tested is shown by the line. The input lines to the membrane module were periodically disconnected, and an ordinary hair dryer was placed at the input line to dry the membrane. When leakage rates were high, drying of the membrane greatly lowered leakage rates.

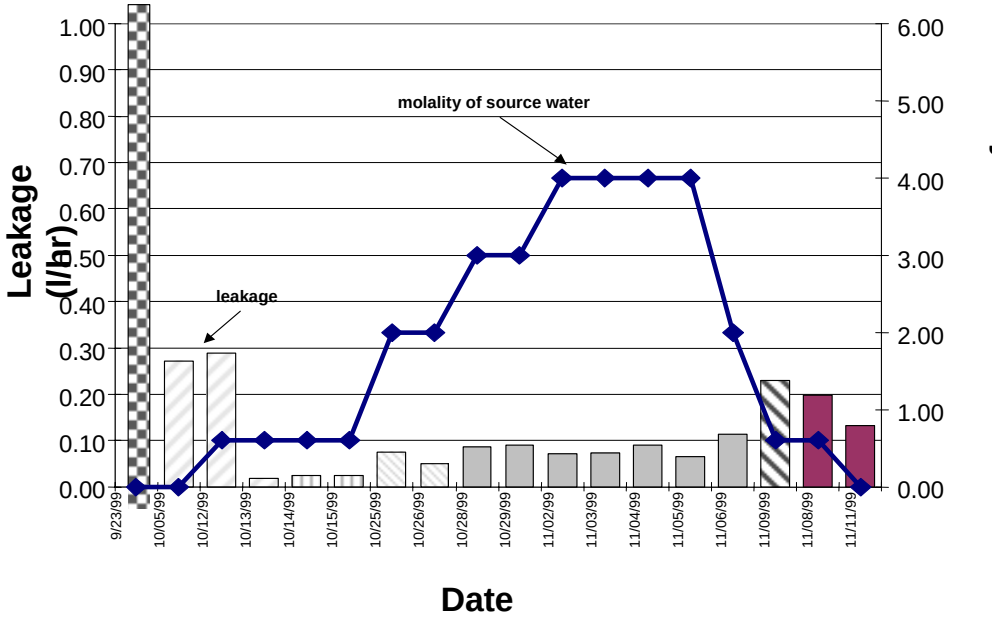

Figure 12. History of membrane leakage.

Figure 13 shows the results for the groundwater tests performed during September. The source water was sequentially concentrated by recycling concentrate into the source tank. Figure 14 is the percent removal of dissolved solids during the tests. The only low percent removal occurred during a day when the temperature drop was reduced to 1.3 ºC. As explained above, at low flux the distillate production declines, while leakage of source water across wetted pores remains constant, leading to net decline in output water quality. Overall, removal efficiency is very high and independent of the concentration of the source water. Although there was no evidence of membrane fouling during the test, additional, longer-term tests are needed to fully evaluate membrane fouling.

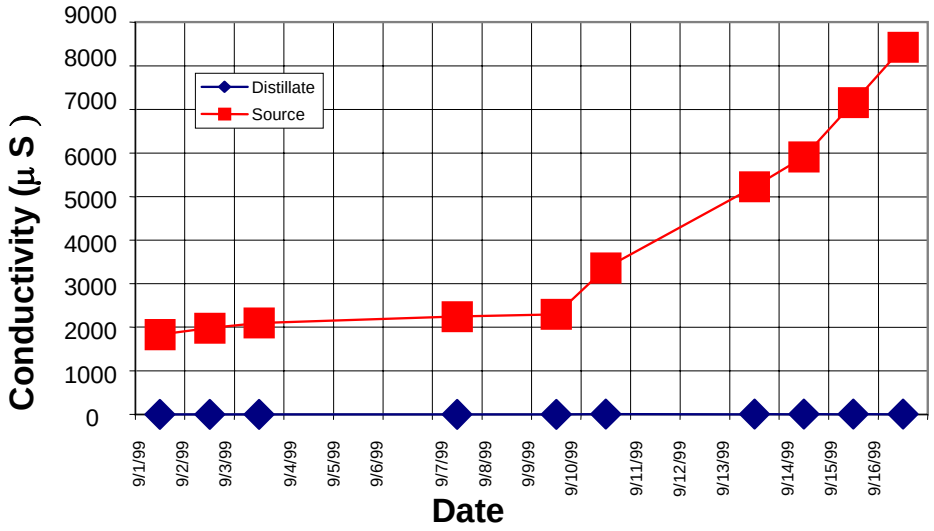

Figure 13. Groundwater results.

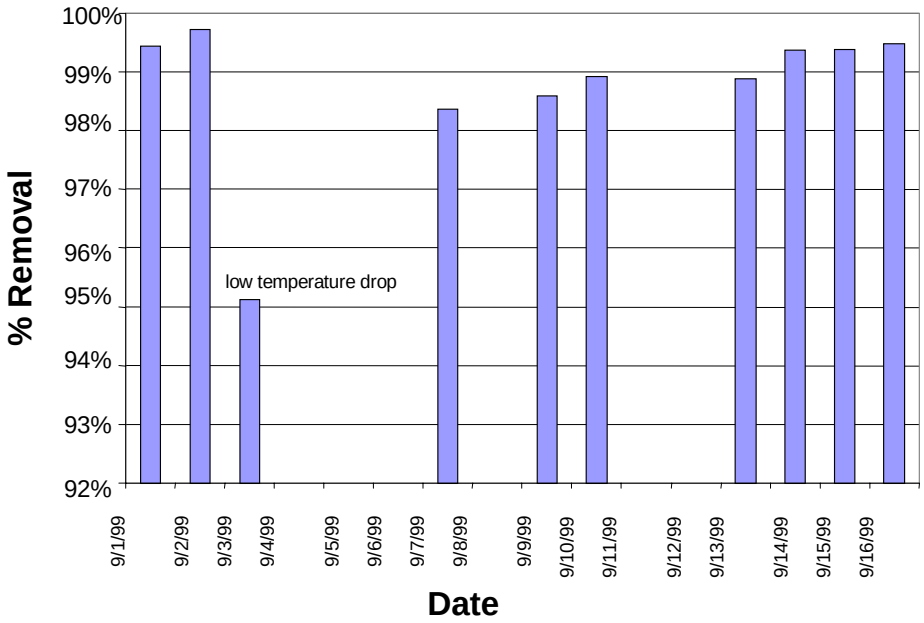

Figure 14. Percent removal of dissolved solids from groundwater.

Operationally, leakage seemed to increase with pressure spikes and lack of a temperature gradient. In one case, the system was left on over the weekend and the cooling loop failed. Upon resumption of normal operation, the leakage rate had increased dramatically. It is suspected that the absence of a temperature gradient led to 100-percent relative humidity throughout the system with resultant pore wetting. During normal operation, evaporation into the air gap helps keep the membrane dry.

Much lower leakage rates would be anticipated under normal operating conditions. Running the hot water through the module at either near zero or zero gage pressure could effectively prevent leakage. The total pressure in the air gap is atmospheric. When the hot water is at or near atmospheric pressure (figure 1), the gradient in total pressure is approximately zero, reducing pressure-induced flow through the wetted pores to zero.

4.0 Analysis

4.1 Variables Controlling System Response

The driving force for membrane distillation is the difference in vapor pressure between the evaporation surface, somewhere inside the membrane, and the cold side. With air gap membrane distillation, one anticipates that flux will be limited by diffusion of water vapor across the air gap. Jonsson, *et al*. (1985) and Lawson and Lloyd (1997) developed mathematical models that describe air gap MD as a vapor diffusion limited process.

The vapor pressure of pure water and brine as a function of temperature is illustrated in figure 15. Note that the vapor pressure curve becomes steeper at higher temperatures. Thus, the change in vapor pressure from hot to cold side, for a given temperature drop, is much greater at higher temperatures. Likewise, the first few degrees of temperature drop provide a much greater change in vapor pressure than further temperature drops. Diffusion coefficients and the diffusional bulk flow term are also greater at higher temperature. If the system were limited by vapor diffusion, the flux rates should be:

- Much higher at higher hot side temperatures (Jonsson, *et al*., 1985; Lawson and Lloyd, 1997)

- Strongly nonlinear with respect to temperature drop, with flux increases dropping off at high temperature drops (Jonsson, *et al*., 1985; Lawson and Lloyd, 1997).

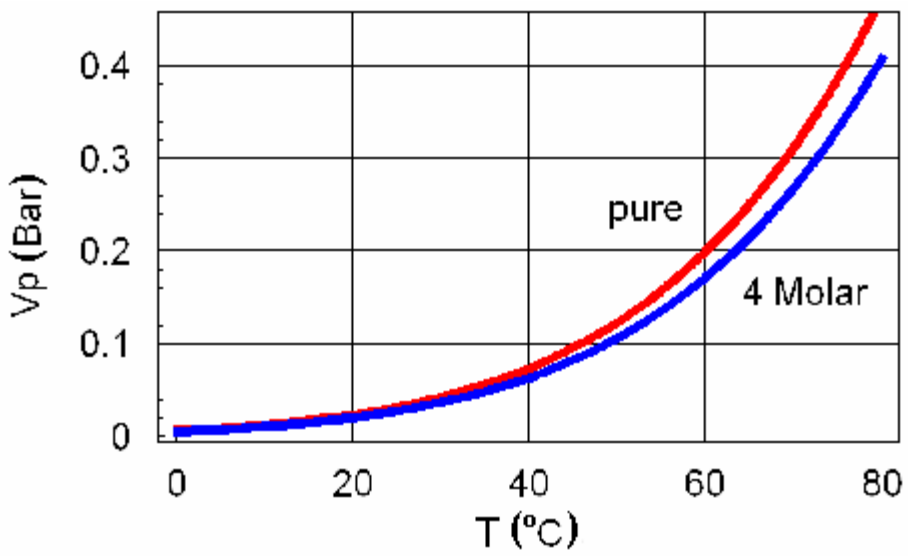

Figure 15. Vapor pressure of pure water and concentrated brine.

Figure 16 illustrates the characteristic shape of vapor diffusion limited flux. The calculation assumes diffusion of saturated water vapor at hot side temperatures of 70, 50, and 30 ºC across a 1-mm air gap. Notice that the curves are not linear (whereas the measured data is linear) and the

large importance of hot side temperature (whereas the measured data has only a weak hot side temperature dependence).

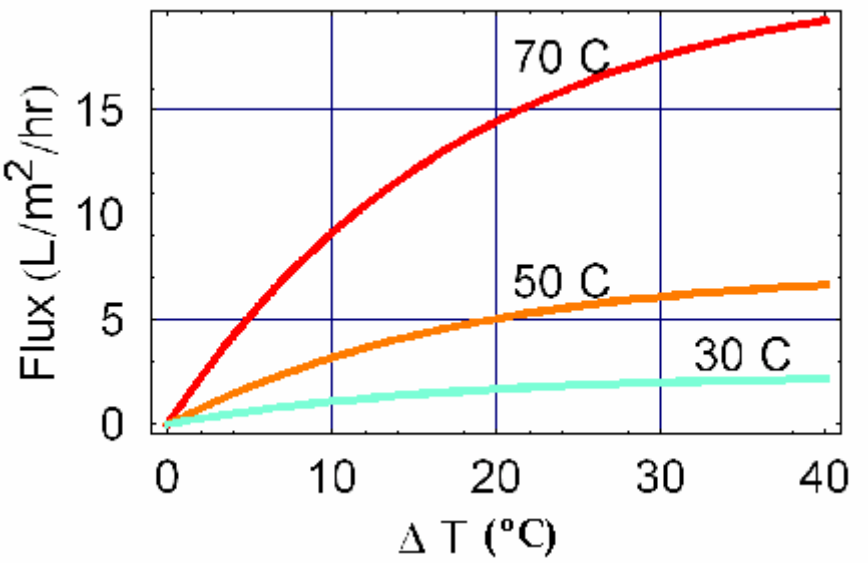

Figure 16. Diffusion of water vapor across a hypothetical 1-mm air gap as a function of temperature drop at three different hot side temperatures.

The influence of salinity on vapor pressure is modest (about a 25-percent lowering in vapor pressure for a saturated sodium chloride solution) and should lead to only small declines in flux. Figure 17 shows the thermodynamic requirement for initiation of flux of brines. Ten percent salinity is approximately 2 M. Comparing the thermodynamic requirements in figure 17 with the x-axis intercepts of the data in figure 6 indicates that flux is initiated at temperature drops well above the thermodynamic minimum. Observed fluxes of brines initiate at much greater temperature drops than required by thermodynamics. However, flux of pure water begins at infinitesimal temperature drops as predicted by thermodynamics, so initiation of flux is at the thermodynamic limit for pure water but at higher than thermodynamically required temperature drops for brines.

The observed behavior of the system suggests that the primary limiting factor flux is heat transfer to the evaporation surface. This type of behavior would be expected for direct contact, but not air gap MD. Heat transfer is linear in temperature drop and does not depend upon hot side temperature. If the system was limited by heat transfer, then flux should increase linearly with temperature drop and be independent of hot side temperature—a good fit to the data. Additionally, in a heat transfer limited system, higher salinity source water would require greater temperature drops across the air gap, leading to more conduction heat losses, more temperature polarization, and lower efficiency. Heat transfer limitation explains the linear behavior with temperature drop, the small dependence upon hot side temperature, and the increased dependence on salinity of the measured data.

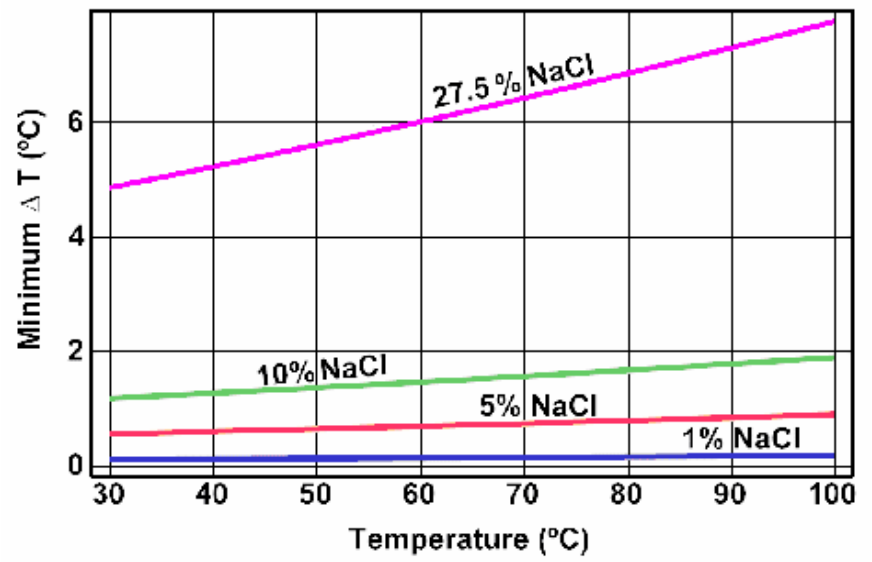

Figure 17. Minimum temperature drop required to begin flux based upon thermodynamic limit.

In summary, the data strongly suggest that flux in this module is primarily limited by heat transfer from the bulk hot solution to the evaporation surface, rather than vapor diffusion as theory would suggest.

4.2 Heat Transfer Limited Model

A simple model assuming heat transfer limitation was derived and fit to the experimental data. The model describes the process as being limited by heat transfer to the evaporation surface:

$$q = H_{wall}\,\Delta T_{wall}$$

$$q = H_{dry}\,\Delta T_{gap} + H_{wet}\,\Delta T_{gap}$$

$$\Delta T = \Delta T_{gap} + \Delta T_{wall}$$

$$\text{efficiency} = (\gamma - \alpha\ \text{molality})$$

$$Flux = \frac{efficiency * q}{\lambda}$$

$$Flux = \frac{H_{wet}\Delta T_{gap}}{\lambda}$$

Where q = the heat flow per unit area (W/m^2)

H_{wall} = the heat combined heat transfer coefficient from the bulk hot liquid to the evaporation surface and from the bulk cold liquid to the condensation surface ($W/m^2/°C$)

ΔT_{wall} = the combined temperature drop from the bulk hot liquid to the evaporation surface and from the bulk cold liquid to the condensation surface (^oC)

H_{dry} = the heat transfer coefficient in the air across the air gap ($W/m^2/°C$)

ΔT_{gap} = the temperature drop across the air gap (^oC)

H_{wet} = the heat transfer coefficient for movement of latent heat across the air gap ($W/m^2/°C$)

ΔT = the total temperature drop between the bulk hot and cold liquid (^oC)

efficiency = the fraction of the heat transfer that goes into distillation

γ = the thermal efficiency for distillation of pure water

α = a fitting term for the influence of salinity on efficiency

molality = the molality of the source water (mole salt/kg water)

Flux = production rate of distillate ($kg/m^2/s$)

λ = the latent heat of vaporization of water (J/kg).

Solving for flux gives:

$$Flux = -\frac{\Delta T * H_{dry} * H_{wall}(molality * \alpha - \gamma)}{(H_{dry} + H_{wall} + H_{wall} * molality * \alpha - H_{wall} * \gamma)\lambda}$$

No dependence on flux on hot side temperature is included in the model; rather, simple heat transfer limitation is assumed. The measured results are compared to the model in figure 18. Considering the wide range of experimental variables and simplicity of the model, the agreement is quite good. The slight bias in the model fit (at the low end, the data are below the 1:1 line; at high flux, the data are above the 1:1 line) reflects factors of secondary importance, such as hot side temperature, that are not included in the simple model. Heat transfer rate is the primary, but not the only, limitation for flux.

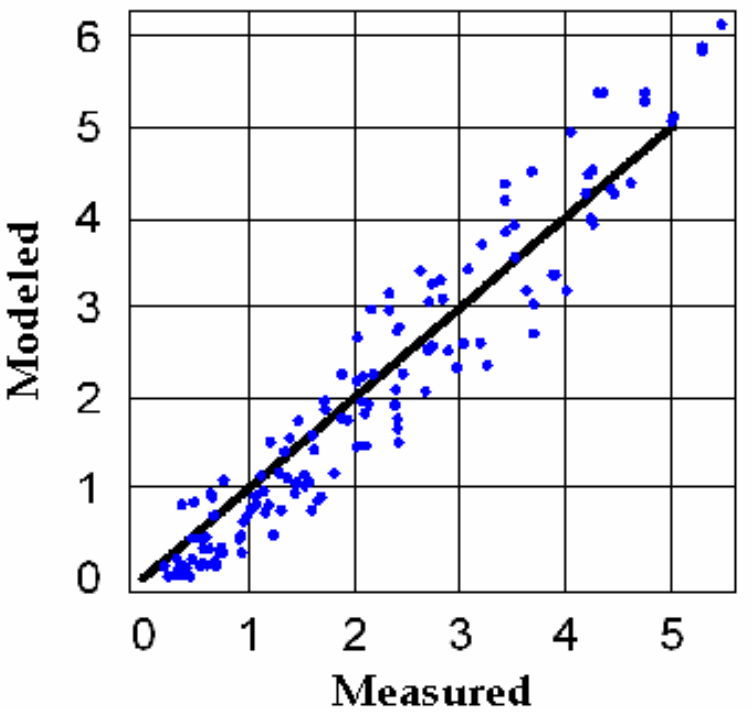

Figure 18. Comparison of measured and modeled results.

The results of the nonlinear curve fit are:

H_{wall}=360,000 (W/m^2/˚C), H_{gap}=34,000 (W/m^2/˚C), α=0.04/molal, and γ=0.94.

The heat transfer coefficient for the gap, which represents lost heat, is much lower than the coefficient for the walls, giving high thermal efficiency. Higher thermal efficiency is a primary benefit of the air gap.

The predicted thermal efficiency of the membrane module is shown in figure 19 as a function of source water salinity. Efficiency declines with salinity because high salinity water requires a greater temperature drop across the air gap, leading to greater heat conduction losses through the air gap. Predicted flux as a function of salinity at two different temperature drops is shown in figure 20. Flux declines significantly at higher salinity.

Temperature polarization is one measure of MD operation. Temperature polarization is defined by Lawson and Lloyd (1997) as the ratio of temperature drop across the air gap to the total temperature drop. A temperature polarization of 1.0 is indicative of a mass transport limited system, whereas lower temperature polarization coefficients indicate the system is limited by heat transfer to the evaporation surface. Figure 21 shows the temperature polarization coefficient, which ranges from 0.4 to 0.7. Concentrated brines have greater mass transfer limitations, based upon their lower vapor pressure. The overall low value of the temperature polarization coefficient explains why flux through the system is not consistent with mass transport limited models. The reason for the low value of the temperature polarization

coefficient is unknown. A hypothesis is that vibrations in the system lead to convection in the air gap. Convection in the air gap would lead to much higher mass transfer coefficients than predicted by molecular diffusion. The high mass transfer coefficients in the air gap would cause the air gap system to behave more like direct contact membrane distillation.

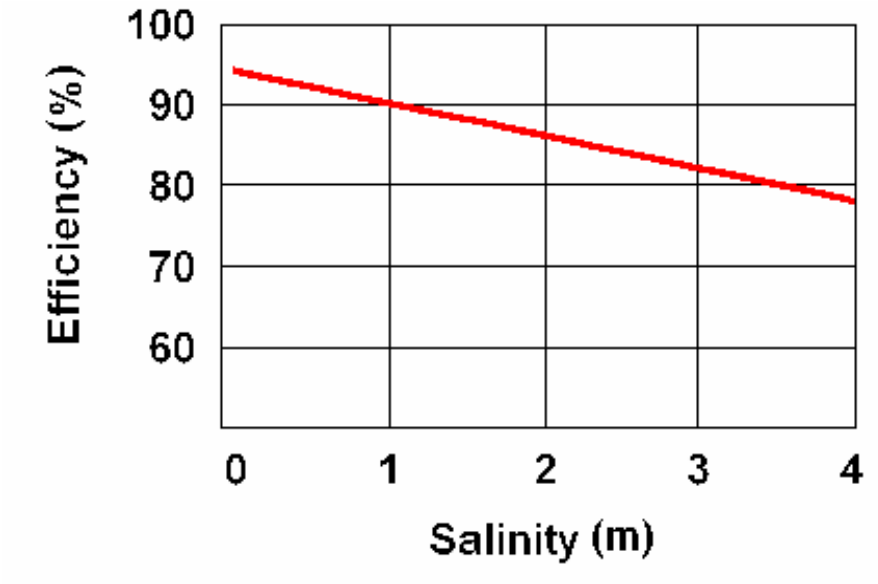

Figure 19. Predicted system efficiency as a function of source water salinity.

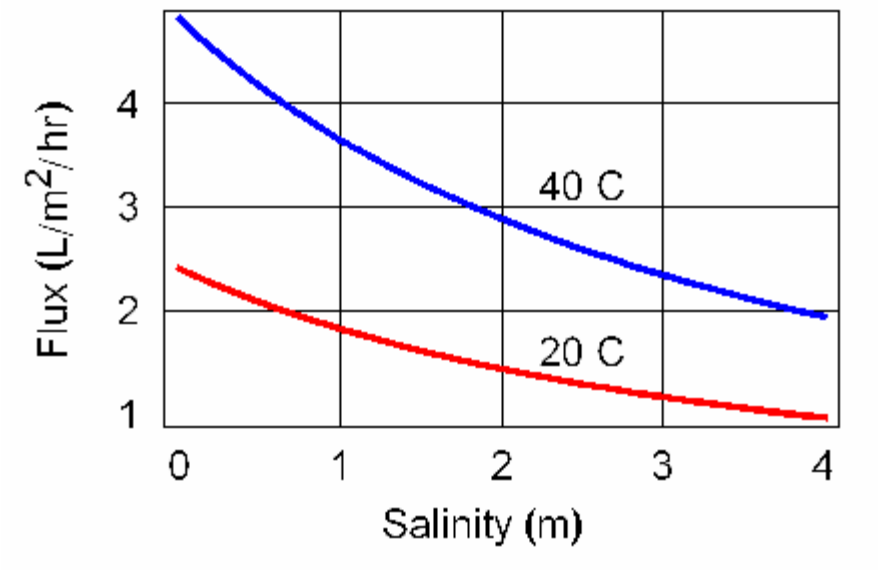

Figure 20. Predicted flux at two temperature drops.

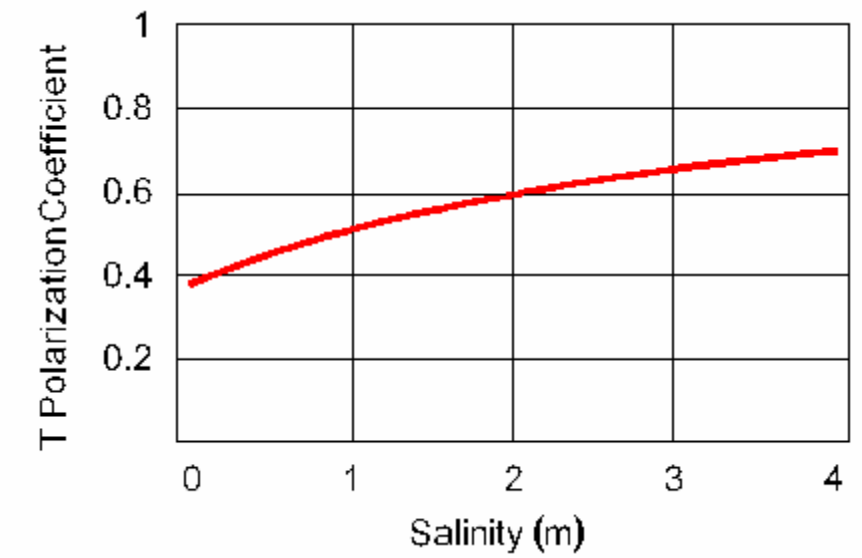

Figure 21. Temperature polarization coefficient for a total temperature drop of 30 ˚C.

Figure 22 gives the predicted temperature drops in the air gap relative to the rest of the system. Higher salinity solutions require a greater temperature drop across the air gap. The higher temperature drop across the air gap leads to greater heat losses by conduction across the air gap (i.e., the portion of heat energy that is wasted).

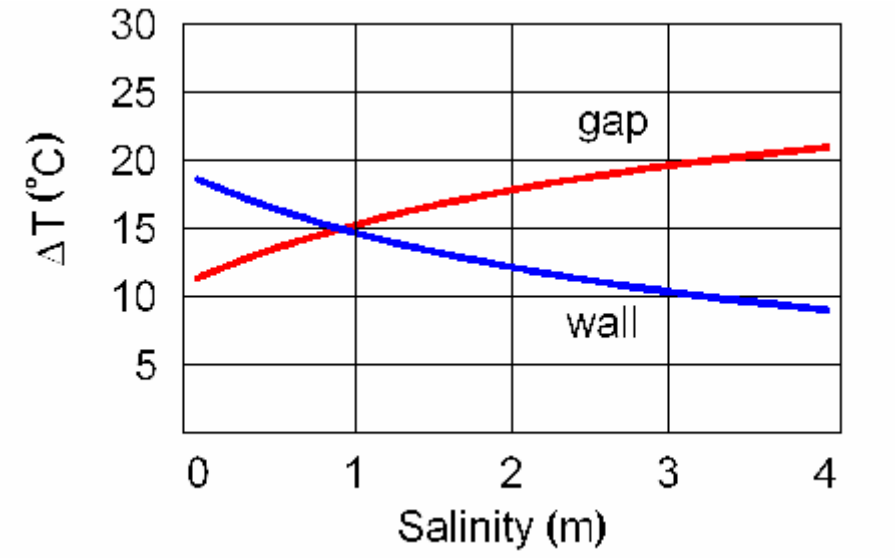

Figure 22. Predicted temperature drop in the system at a total temperature drop of 30 ˚C.

4.3 Projected Efficiency of Membrane Distillation

The module tested was not designed to recover the latent heat of vaporization, a necessary requirement for high overall thermal efficiency. The commercial technology for membrane distillation is in an early stage, and the logical first step is to produce working, reliable membrane modules. Thermal efficiency of MD can be increased by going to a countercurrent flow system, such as shown by Bier and Plantikow (1995).

Figure 23 shows the countercurrent flow schematic. Cold water comes in at the bottom and is gradually warmed by the latent heat of condensation. At the end of the cool side, additional heat energy is added to the water, making it appropriate for the hot side. The additional heat could come from any source. The schematic shows a solar collector. Solar collectors are very efficient at the low temperatures required for membrane distillation. Water on the hot side cools along the flow path as latent heat is removed. Figure 24 shows the economy ratio for such a system, assuming 90 percent of the energy goes into desalination (the unit measured had about a 95-percent thermal efficiency). Each line represents a different transmembrane temperature drop. The abscissa is the total temperature change on either side (hot-cool) in figure 23. The performance lines are linear because the thermal energy is stored in the liquid water with an effectively constant heat capacity.

Figure 25 shows a comparison between economy ratio for MD and the dewvaporation process (Beckman and Hamieh, 1999), another promising thermal technology. Dewvaporation works by evaporation of water on the cold side of a film, followed by condensation on the warm side. The thermal energy is carried through the system primarily in the gas phase. The calculation assumes a hot side temperature of 80 ºC and a transmembrane (or trans wall for dewvaporation) temperature drop of 5 ºC. One hundred percent efficiency is assumed for dewvaporation, and 90-percent efficiency is assumed for membrane distillation. In practice, it is much more difficult to obtain the theoretical maximum efficiency with dewvaporation. Although comparison is shown for only one set of parameters, the difference occurs in general. Over every set of identical operating parameters, MD has a thermodynamic edge over dewvaporation. The difference is caused by the nonlinearity in the water vapor pressure equation. Air holds much more water vapor at higher temperatures, the point where heat addition occurs in dewvaporation. In contrast, for membrane distillation the heat energy is stored in the water, giving efficiencies that are linearly related to temperature drop.

Thomas (1997) cites energy use of multistage flash distillation as ranging from 48 to 441 kWh/m^3 with an average of 60 to 80 kWh/m^3. For multi-effect distillation, approximately 30 kWh/m^3 of thermal energy is required (Thomas, 1997). Energy requirements for reverse osmosis range from 3 kWh/m^3 for brackish water to 17 kWh/m^3 for seawater (Thomas, 1997). With energy recovery, seawater reverse osmosis energy used declines to 5 to 6 kWh/m^3 (Thomas, 1997). Glueckstern (1995) estimates energy use for hybrid multi-effect distillation and reverse osmosis of seawater as 5.5 to 6.5 kWh/m^3. Energy use for reverse osmosis is electricity, which is more expensive than low-grade thermal energy. Assuming an economy ratio of 15, membrane distillation has an energy use of 44 kWh/m^3. Thus, MD is competitive energetically

with other thermal desalination technologies. Additionally, MD can operate at hot side temperatures much lower than other thermal desalination technologies and is dramatically simpler.

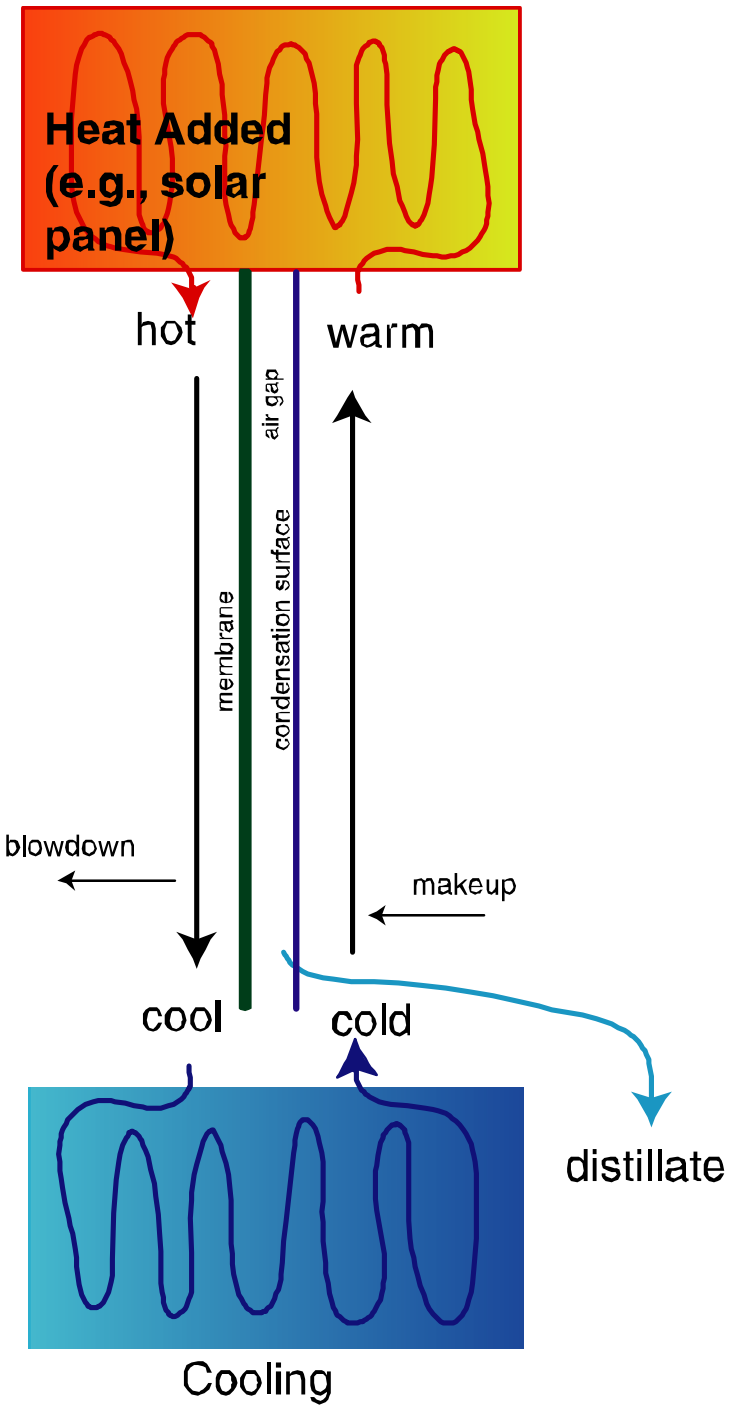

Figure 23. Membrane distillation with heat recovery.

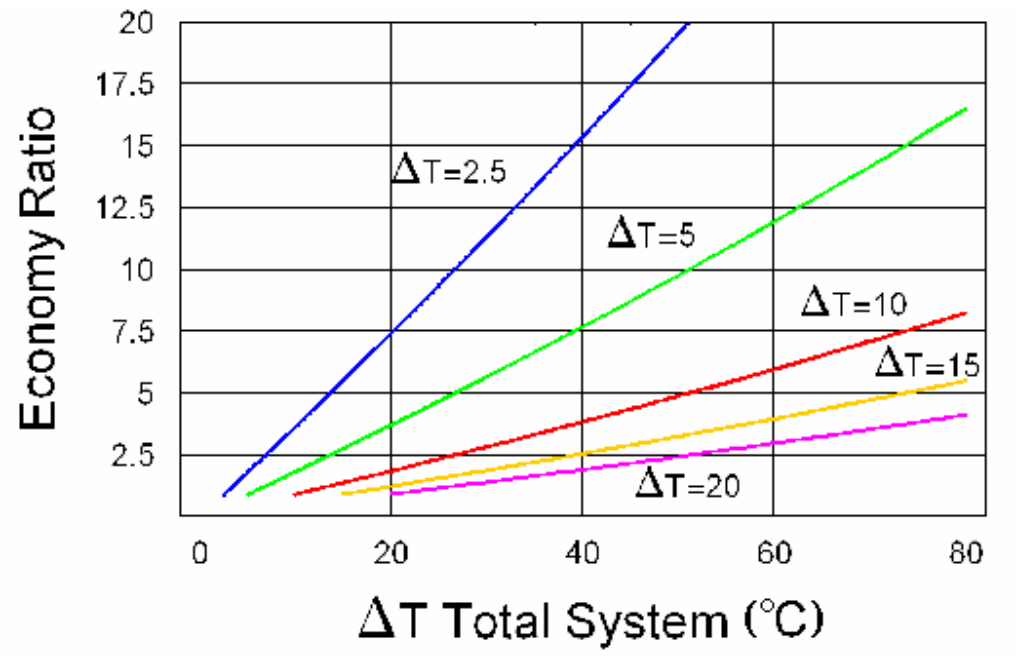

Figure 24. Economy ratio (heat energy used for desalination/total heat energy input) at different transmembrane temperature drops.

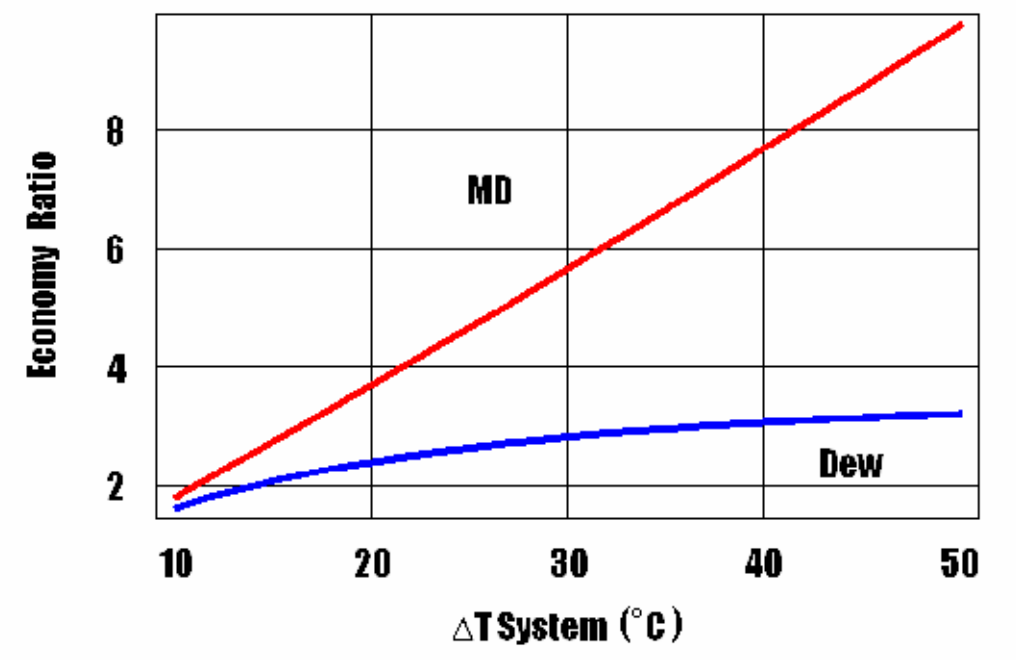

Figure 25. Comparison of membrane distillation and dewvaporation at a hot side temperature of 80 ˚C and a temperature drop of 5 ˚C.

Capital expenses are difficult to estimate since no large-scale MD systems have ever been built. In comparison to reverse osmosis, when fully developed, MD should be significantly lower in capital and operational expenses. Membrane distillation operates best at very low pressures, allowing for thinner piping and fewer problems with leaks and pump failure.

Assuming the capital cost of a membrane distillation facility is 0.375 $/m^3 (same as sea water reverse osmosis), the total cost as a function of thermal energy cost is given in table 2. The table assumes a fully developed MD industry (which currently does not exist). The energy cost for reverse osmosis is assumed to be 0.375 $/m^3 (Wangnick, 2000). For comparison, the cost of natural gas is around 0.025 $/kWh and the cost of energy from large solar ponds ranges from 0.005 to 0.015 $/kWh (Esquivel, 1992). Membrane distillation is only competitive relative to reverse osmosis when low cost heat energy is available and/or when the water chemistry of the source water is too difficult for treatment with reverse osmosis.

Table 2. Cost estimate for fully developed membrane distillation treatment

Thermal energy cost ($/kWh)	MD cost ($/m^3)	MD/RO cost
Free	0.375	0.5
0.0025	0.485	0.65
0.005	0.595	0.79
0.0075	0.705	0.94
0.01	0.815	1.09
0.0125	0.925	1.23
0.015	1.035	1.38
0.0175	1.145	1.53
0.02	1.255	1.67

The major advantages of membrane distillation are: (a) greater simplicity (gravity flow through the membrane module with minimal pretreatment is all that is required); (b) use of very low grade heat (down to 13 °C or below); and (c) the ability to treat highly concentrated brines. Membrane distillation can be cost competitive in several areas:

- For further treatment of reverse osmosis concentrate
- For isolated applications using solar energy
- For waste heat applications
- With geothermal waters
- For mobile military applications

References

Banat, F.A., and J. Simandl, "Theoretical and Experimental Study in Membrane Distillation," *Desalination Journal*, 95, pp. 39-52, 1994.

Bandini, S., C. Gostoli, and G.C. Sarti, *Role of Heat and Mass Transfer in Membrane Distillation Process, Desalination and Water Re-Use*, Proceedings of the Twelfth International Symposium, pp. 91-106, 1991.

Beckman, J.R., and B.M. Hamieh, *Desalination by Dewvaporation Process*, Proceedings of 1999 International Desalination Association World Congress, San Diego, California, August 1999.

Bier, C., and U. Plantikow, *Solar-Powered Desalination by Membrane Distillation*, IDA World Congress on Desalination and Water Sciences, Abu Dhabi, November 18-24, 1995 <http://www2.hawaii.edu/~nabil/solar.htm>.

Chemical Rubber Co., *Handbook of Chemistry and Physics*, 50th edition, Cleveland, Ohio, 1970.

Donovan, Robert, and Dennis Morrison, "Evaluation of Membrane Distillation Prototypes for Use in Semiconductor Manufacturing," unpublished final report prepared by Sandia National Laboratory as part of a water conservation project sponsored jointly by the U.S. Environmental Protection Agency, Department of Energy, and SEMATECH, 1998.

Esquivel, P.M., *Economic Feasibility of Utilizing Solar Pond Technology to Produce Industrial Process Heat, Base Load Electricity, and Desalted Brackish Water*, Masters Thesis, University of Texas at El Paso, 1992.

Glueckstern, P., "Potential Uses of Solar Energy for Seawater Desalination," *Desalination*, 101, pp. 11-20, 1995.

Hogan, P., A. Sudjito, A.G. Fane, and G.L. Morrison, *Desalination by Solar Heated Membrane Distillation, Desalination and Water Re-Use*, Proceedings of the Twelfth International Symposium, pp. 81-90, 1991.

Jonsson, A.S., R. Wimmerstedt, and A.C. Harrysson, "Membrane Distillation - A Theoretical Study of Evaporation Through Microporous Membranes," *Desalination*, 56, pp. 247-249, 1985.

Lawson, K.W., and D.R. Lloyd, "Membrane Distillation," *Journal of Membrane Science*, 124, pp. 1-25, 1997.

Lawson, K.W., *Membrane Distillation*, Ph.D. Dissertation, University of Texas at Austin, UMI Microform 9603893, 1995.

Ohta, K., I. Hayano, T. Okabe, T. Goto, S. Kimura, and H. Ohya, *Membrane Distillation with Fluoro-carbon Membranes, Desalination and Water Re-Use*, Proceedings of the Twelfth International Symposium, pp. 107-115, 1991.

Solis, Sergio, *Water Desalination by Membrane Distillation Coupled with a Solar Pond*, Masters Thesis, Department of Civil Engineering, University of Texas at El Paso, 1999.

Thomas, K.E., *Overview of Village Scale, Renewable Energy Powered Desalination*, NREL/TP-440-22083, UC Category: 1210 DE 97000240, 1997.

Wangnick, Klaus, Present Status of Thermal Seawater Desalination Techniques, *Desalination and Water Reuse Quarterly*, Vol. 10, No. 1. p. 14-21, 2000.

APPENDICES

Appendix A

Performance Data for October 5, 1999

Performance data for 10/05/99 at 4.8 gpm flow rate.

Time	Hot in Mem (°C)	Cold in Mem (°C)	Delta T (°C)	Prod Rate (gph)	Feed Cond (µS/cm)	Prod Cond (µS/cm)
4:06 PM	71.60	39.40	32.2	2.6130	245	4.87
4:01 PM	71.70	39.30	32.4	2.6130	243	4.62
3:46 PM	71.60	36.40	35.2	3.0881	240	4.34
3:40 PM	71.40	36.00	35.4	3.0485	238	4.27
3:30 PM	71.90	35.10	36.8	3.3490	235	4.20
3:22 PM	72.10	35.00	37.1	3.3025	231	4.16
2:48 PM	71.10	32.70	38.4	3.3969	213	3.73
2:24 PM	70.50	28.80	41.7	3.9630	203	3.70

Appendix B

Experimental Data for November 11-12, 1999

Experimental data for 11/11/99 at 5.5 gpm flow rate.

	Hot in	Cold in	Delta T	Prod Rate	Flux Rate	Feed Cond	Prod Cond
Time	(°C)	(°C)	(°C)	(gph)	($L/m^2/h$)	(µS/cm)	(µS/cm)
2:44 PM	67.0	25.4	41.6	3.9286	5.0030	485	5.25
3:09 PM	67.0	32.2	34.8	3.3119	4.2117	485	5.92
3:32 PM	67.2	38.0	29.2	3.0293	3.8449	485	6.85
3:54 PM	67.1	43.5	23.6	2.4035	3.0387	485	8.71
4:16 PM	67.6	52.0	15.6	1.7501	2.2055	485	10.25
4:30 PM	68.0	58.0	10.0	1.1745	1.4737	485	12.30
4:56 PM	68.0	62.6	5.4	0.7015	0.8538	485	26.50
5:12 PM	66.4	62.4	4.0	0.6499	0.7868	485	28.92
6:24 PM	54.1	23.4	30.7	2.3534	2.9663	485	10.16
6:51 PM	54.2	29.0	25.2	2.0185	2.4958	485	19.19
7:20 PM	54.4	34.0	20.4	1.7613	2.1525	485	24.60
7:37 PM	55.1	39.0	16.1	1.3546	1.6450	485	27.50
7:57 PM	56.1	45.0	11.1	1.0829	1.3056	485	30.80
8:43 PM	58.2	52.9	5.3	0.7189	0.8341	485	47.90
9:06 PM	47.0	22.3	24.7	1.8090	2.2776	525	11.57
9:17 PM	46.6	29.3	17.3	1.5139	1.6442	525	82.10
9:27 PM	46.7	33.4	13.3	1.2285	1.1475	525	144.10
9:43 PM	46.8	40.5	6.3	0.8377	0.7395	525	165.00
9:59 PM	46.0	43.0	3.0	0.6287	0.4903	525	207.00

Experimental data for 11/11-12/99 at 11 gpm flow rate.

Time	Hot in Mem (°C)	Cold in Mem (°C)	Delta T (°C)	Prod Rate (gph)	Flux Rate ($L/m^2/h$)	Feed Cond (µS/cm)	Prod Cond (µS/cm)
11:16 PM	68.3	26.2	42.1	5.3263	5.9327	560	75.50
11:28 PM	67.5	33.0	34.5	4.4076	4.8202	560	84.30
11:43 PM	68.3	38.2	30.1	4.0113	4.2863	560	95.20
11:57 PM	68.2	42.4	25.8	3.5667	3.6923	560	109.70
12:06 AM	67.7	47.5	20.2	2.9425	2.9426	560	125.00
12:13 AM	68.3	52.9	15.4	2.4935	2.4592	560	131.00
12:22 AM	69.0	57.5	11.5	2.0502	1.8608	560	165.20
12:41 AM	67.8	61.3	6.5	1.6186	1.3292	560	202.80
1:04 AM	67.4	64.1	3.3	1.2703	0.8454	560	270.50
11:47 AM	57.0	24.0	33.0	3.4522	3.6240	740	136.60
11:58 AM	56.4	27.8	28.6	3.1977	3.2778	740	150.80
12:16 PM	56.0	32.5	23.5	2.7669	2.7270	740	173.50
1:10 PM	57.5	42.5	15.0	2.1513	1.9032	740	231.50
1:29 PM	58.3	45.4	12.9	1.9815	1.6775	740	253.40
1:44 PM	59.0	49.6	9.4	1.5907	1.2730	740	280.00
2:19 PM	57.1	53.3	3.8	1.0823	0.6590	740	390.00
2:40 PM	47.6	23.3	24.3	2.0396	2.1968	800	130.70
2:49 PM	45.6	27.8	17.8	1.8828	1.8074	800	203.50
2:59 PM	47.1	33.6	13.5	1.6814	1.4184	800	275.80
3:10 PM	46.5	39.6	6.9	1.0592	0.8097	800	325.00
3:18 PM	45.5	42.8	2.7	0.9315	0.6506	800	366.00

Experimental data for 11/12/99 at 15.5 and 20.5 gpm flow rates.

Time	Hot in Mem (°C)	Cold in Mem (°C)	Delta T (°C)	Prod Rate (gph)	Flux Rate ($L/m^2/h$)	Feed Cond (µS/cm)	Prod Cond (µS/cm)
15.5 gpm							
4:22 PM	69.6	28.5	41.1	6.8340	6.7032	850	202.40
4:33 PM	67.4	37.6	29.8	5.3151	4.8704	850	245.00
4:55 PM	66.3	45.6	20.7	4.2368	3.3048	850	335.00
5:05 PM	66.9	56.2	10.7	3.1486	2.2414	850	380.00
5:25 PM	68.0	64.1	3.9	2.4164	1.1272	850	542.00
20.5 gpm							
6:12 PM	69.1	28.5	40.6	7.3712	6.7124	900	263.40
6:20 PM	68.7	33.6	35.1	6.3861	5.4080	900	308.00
6:30 PM	66.3	35.5	30.8	6.0347	4.7306	900	352.00
6:49 PM	67.6	41.6	26.0	5.3735	3.8740	900	396.00
7:27 PM	66.7	49.0	17.7	4.7056	2.8204	900	481.00
7:39 PM	65.9	56.2	9.7	3.8045	1.7850	900	572.00
7:50 PM	66.4	59.9	6.5	3.5850	1.3333	900	640.00
8:06 PM	67.0	63.1	3.9	3.4387	0.9002	900	717.00

Appendix C

Performance for Salt Concentrations

Performance for salt concentration M=0.6, S.G.=1.025 at 5.5 gpm flow rate.

Time	Hot in Mem (°C)	Cold in Mem (°C)	Delta T (°C)	Prod Rate (gph)	Flux Rate ($L/m^2/h$)	Feed Cond (mS/cm)	Prod Cond (µS/cm)
10/14/99							
12:10 PM	76.00	33.50	42.5	4.1716	5.3627	71.200	105.00
12:38 PM	76.00	33.00	43.0	4.1716	5.3641	71.200	86.00
1:35 PM	75.00	35.00	40.0	3.8352	4.9304	71.200	101.70
1:50 PM	76.00	39.70	36.3	3.4968	4.4948	71.200	110.70
2:46 PM	76.70	50.00	26.7	2.3778	3.0538	71.200	172.10
3:05 PM	77.00	60.00	17.0	1.4411	1.8473	71.200	305.00
3:13 PM	77.00	66.00	11.0	0.8782	1.1197	71.200	689.00
3:18 PM	77.00	67.00	10.0	0.5859	0.7447	71.200	909.00
11/08/99							
12:21 PM	67.50	25.50	42.0	3.5061	4.4277	73.000	1392.00
12:55 PM	67.30	32.50	34.8	2.7583	3.4666	73.000	1737.00
1:41 PM	66.90	36.50	30.4	2.6496	3.3114	73.000	2135.00
2:09 PM	66.10	45.60	20.5	1.7332	2.1375	73.000	3070.00
2:20 PM	66.70	53.00	13.7	1.2048	1.4523	73.000	4650.00
3:03 PM	67.90	61.30	6.6	0.5310	0.5903	73.000	9960.00
3:24 PM	66.70	62.10	4.6	0.3408	0.3541	73.000	14080.00
4:18 PM	55.40	23.90	31.5	2.0211	2.5143	73.000	2460.00
4:38 PM	54.60	28.20	26.4	1.6063	1.9938	73.000	2620.00
5:07 PM	56.20	35.50	20.7	1.4161	1.7504	73.000	2910.00
5:30 PM	57.30	44.60	12.7	0.9036	1.0801	73.000	5220.00
5:55 PM	56.60	51.20	5.4	0.3329	0.3566	73.000	12260.00
11/09/99							
12:04 PM	60.20	24.40	35.8	2.4729	3.1140	73.000	1598.00
12:58 PM	47.60	23.70	23.9	1.1631	1.4246	73.000	3550.00
1:05 PM	44.80	28.50	16.3	0.6658	0.7805	73.000	6530.00
1:19 PM	43.50	34.50	9.0	0.3276	0.3612	73.000	10480.00
1:34 PM	44.40	38.80	5.6	0.2446	0.2516	73.000	14680.00
1:42 PM	43.60	40.50	3.1	0.1585	0.1442	73.000	21420.00
1:54 PM	42.80	40.80	2.0	0.0981	0.0597	73.000	38480.00

Performance for salt concentration M=2.0 with S.G.=1.083 at 5.5 gpm flow rate.

Time	Hot in Mem (°C)	Cold in Mem (°C)	Delta T (°C)	Prod Rate (gph)	Flux Rate ($L/m^2/h$)	Feed Cond (mS/cm)	Prod Cond (µS/cm)
10/25/99							
2:30 PM	73.3	25.9	47.4	3.3900	4.3360	173.200	1124.00
3:09 PM	73.6	26.2	47.4	3.2500	4.1558	177.900	1202.00
3:36 PM	73.7	26.1	47.6	2.9723	3.8010	179.900	1203.00
4:00 PM	73.7	29.2	44.5	2.8648	3.6583	184.200	1495.00
4:31 PM	72.8	33.8	39.0	2.5568	3.2605	177.800	1682.00
4:53 PM	73.7	35.7	38.0	2.5296	3.2325	171.300	1270.00
5:31 PM	73.2	39.6	33.6	2.1616	2.7598	169.400	1403.00
5:48 PM	73.1	39.8	33.3	2.1230	2.7067	168.900	1635.00
6:12 PM	73.2	43.0	30.2	1.7484	2.2295	168.200	1598.00
6:28 PM	73.3	50.9	22.4	1.1008	1.3961	167.000	2480.00
6:40 PM	73.5	54.6	18.9	0.8551	1.0772	170.300	3660.00
11/06/99							
12:03 PM	61.10	23.10	38.0	1.9974	2.5323	172.000	2620.00
12:47 PM	55.30	22.30	33.0	1.4838	1.8566	172.000	4830.00
1:19 PM	53.80	24.60	29.2	1.1334	1.4169	172.000	4980.00
2:52 PM	54.80	33.60	21.2	0.7926	0.9789	172.000	6990.00
3:26 PM	56.00	42.80	13.2	0.4835	0.5880	172.000	9530.00
4:01 PM	54.90	46.20	8.7	0.2473	0.2817	172.000	19840.00
4:22 PM	54.20	49.00	5.2	0.1078	0.1148	172.000	29720.00
4:44 PM	46.00	22.70	23.3	0.6975	0.8579	172.000	7680.00
4:51 PM	42.80	30.00	12.8	0.3646	0.4418	172.000	10110.00
5:00 PM	41.50	33.80	7.7	0.1268	0.1481	172.000	15980.00
5:05 PM	41.10	35.50	5.6	0.0922	0.0989	172.000	28700.00
5:14 PM	40.70	36.20	4.5	0.0713	0.0712	172.000	38550.00

Performance for salt concentration M=3.0 with S.G.=1.118 at 5 gpm flow rate.

Time	Hot in Mem (°C)	Cold in Mem (°C)	Delta T (°C)	Prod Rate (gph)	Flux Rate ($L/m^2/h$)	Feed Cond (mS/cm)	Prod Cond (µS/cm)
10/28/99							
12:42 PM	71.7	25.5	46.2	1.9651	2.5022	220.0	2410.0
12:52 PM	71.5	25.6	45.9	1.9651	2.5020	220.6	2430.0
1:16 PM	72.4	31.6	40.8	1.6115	2.0466	221.2	2995.0
1:38 PM	72.4	37.9	34.5	1.1251	1.4201	219.6	4295.0
2:06 PM	73.0	45.8	27.2	0.5860	0.7215	220.7	9620.0
2:41 PM	73.8	52.8	21.0	0.3662	0.4410	220.9	14290.0
3:41 PM	68.0	55.6	12.4	0.2226	0.2647	219.0	16750.0
3:48 PM	66.3	54.6	11.7	0.1025	0.1184	219.0	22460.0
10/29/99							
12:53 PM	70.6	25.9	44.7	2.6449	3.3673	221.5	2460.0
1:31 PM	65.4	29.0	36.4	1.4942	1.8915	223.1	3730.0
2:10 PM	65.5	38.7	26.8	0.8203	1.0277	222.5	5970.0
2:53 PM	64.0	41.7	22.3	0.5860	0.7143	223.1	11870.0
3:22 PM	61.0	51.9	9.1	0.0976	0.1011	222.4	43530.0

Performance for salt concentration M=4.0, S.G.=1.171 at 5 gpm flow rate.

Time	Hot in Mem (°C)	Cold in Mem (°C)	Delta T (°C)	Prod Rate (gph)	Flux Rate ($L/m^2/h$)	Feed Cond (mS/cm)	Prod Cond (µS/cm)
11/02/99							
12:12 PM	71.0	23.2	47.8	2.4470	3.1260	258.000	1992.00
1:43 PM	71.4	26.9	44.5	2.3073	2.9445	258.000	2255.00
2:20 PM	72.2	42.0	30.2	1.3478	1.7120	258.000	3450.00
2:42 PM	72.8	50.8	22.0	0.6328	0.7912	258.000	7420.00
3:10 PM	72.8	57.6	15.2	0.2637	0.3168	258.000	17245.00
3:47 PM	69.3	55.3	14.0	0.1401	0.1572	258.000	33160.00
11/03/99							
12:36 PM	70.5	22.7	47.8	2.3038	2.9324	259.000	2930.00
1:18 PM	70.2	28.5	41.7	2.0648	2.6242	259.000	3320.00
1:44 PM	67.5	32.3	35.2	1.5235	1.9338	259.000	3646.00
2:27 PM	66.0	42.6	23.4	0.7422	0.9255	259.000	8150.00
2:44 PM	66.4	51.0	15.4	0.2131	0.2541	259.000	19130.00
3:19 PM	65.0	56.0	9.0	0.0146	0.0087	259.000	139020.0
3:40 PM	62.3	57.5	4.8	0.0146	0.0000	259.000	258660.0
11/04/99							
12:22 PM	63.8	22.2	41.6	1.6930	2.1524	259.000	3230.00
2:00 PM	52.7	21.4	31.3	0.8877	1.1071	259.000	8090.00
2:29 PM	53.1	28.7	24.4	0.6262	0.7793	259.000	8620.00
3:02 PM	55.6	41.8	13.8	0.1308	0.1292	259.000	60320.00
3:32 PM	55.5	49.2	6.3	0.0282	0.0105	259.000	184050.0
11/05/99							
12:49 PM	61.4	22.9	38.5	1.3712	1.7427	259.000	3310.00
1:17 PM	51.5	21.9	29.6	0.7247	0.9014	259.000	8770.00
1:32 PM	46.0	22.2	23.8	0.5636	0.6926	259.000	11760.00
1:40 PM	43.0	23.9	19.1	0.2140	0.2448	259.000	28840.00
1:50 PM	40.8	28.4	12.4	0.1110	0.1183	259.000	44660.00
2:01 PM	39.7	32.3	7.4	0.0317	0.0315	259.000	58880.00
2:20 PM	39.3	34.5	4.8	0.0108	0.0002	259.000	254500.0

Appendix D

Experimental Data for December 17, 1999

Experimental data for 12/17/99 at low temperatures, M=0, 5 gpm flow rate.

12/17/99			Product Rate				
	Cold in Mem	Delta T	Mem leak	Corrected	Flux Rate	Feed Cond	Prod Cond
Time	(°C)	(°C)	(gph)	(gph)	($L/m^2/h$)	(µS/cm)	(µS/cm)
4:25 PM	13.4	23.1	0.0223	1.233	1.587	1350	24.00
11:34 AM	13.4	20.2	0.0180	0.972	1.252	1350	24.57
12:15 PM	12.4	13.8	0.0089	0.403	0.519	1350	29.24
12:38 PM	12.0	10.6	0.0104	0.361	0.465	1350	37.90
1:05 PM	11.7	7.6	0.0100	0.269	0.346	1350	48.20
1:35 PM	11.7	5.5	0.0175	0.192	0.247	1350	113.00
2:08 PM	11.6	4.2	0.0151	0.111	0.143	1350	162.00
3:08 PM	11.4	1.5	0.0080	0.061	0.078	1350	156.60